2009 American Control Conference
Hyatt Regency Riverfront, St. Louis, MO, USA
June 10-12, 2009

Controlling active cabin suspensions in commercial vehicles

Willem-Jan Evers, Igo Besselink, Arjan Teerhuis, Albert van der Knaap and Henk Nijmeijer

Abstract— **The field of automotive suspensions is changing. Semi-active and active suspensions are starting to become viable options for vehicle designers. Suspension design for commercial vehicles is especially interesting given its potential. An active cabin suspension for a heavy-duty truck is considered, consisting of four ideal actuators with parallel springs, one acting on each corner of the cabin. The main question is how to control this suspension such that it gives optimal comfort when driving in a straight line, but still follows a specified compensation strategy when cornering, braking or accelerating. The proposed controller uses modal input-output-decoupling. Each of the modes has a separate controller including: a skyhook part for enhanced comfort; and an event part for attitude control. The proposed control strategy is tested in simulation using a validated tractor semi-trailer model with idealized actuators. It is shown that driver comfort can be greatly enhanced, without impairing the attitude behavior of the cabin. Furthermore, in contrast to what is known from quarter car analysis, it is shown that adding passive damping is highly desirable.**

I. Introduction

The last few decades, the topic of controller design for (semi-) active vehicle suspensions has received considerable attention, see for example [7], [15]. In contrast to active suspensions, the number of luxury cars with semi-active suspensions is quickly increasing. Semi-active suspensions have a relatively low power consumption and outperform existing passive suspensions. However, the performance is far less than what is achievable with an active suspension, [4]. In addition, the number of control possibilities when cornering, braking and accelerating are also more limited. Why do semi-active suspensions have the preference? The simple answer is: power consumption. The only market ready active devices are based on hydraulic or hydro-pneumatic systems which require significantly more energy.

Real world applications of active suspensions in trucks are limited. One successful implementation is presented in [13]. The experimental platform consists of a tractor semi-trailer with hydraulic (roll) actuators on all the trailer axis as well as on the rear axle of the tractor. Moreover, semi-active dampers are added in the primary (axle) suspension of the tractor. One of the conclusions is that the semi-active dampers only marginally enhance the driver comfort and that the high overall energy consumption (due to the hydraulic actuators) is not feasible within a commercial setting. Hence, when working on driver comfort one should focus on the secondary (cabin) suspension.

In the future electro-mechanic actuators are expected to be a viable solution, [10]. In [3] the clear advantage of active suspensions with (electro-mechanic) energy regenerative actuators is shown. Moreover, it is argued that the use of a so-called *variable geometry active suspension* will further reduce the energy requirements. When applying such a device to the secondary suspension of commercial vehicles, the energy requirements may be lowered to more acceptable values. However, as mentioned in [1], the fields of suspension control for commercial vehicles and in particular design and control of secondary suspensions, are little addressed in literature.

A relevant approach to the control of secondary suspensions is given in [11], [12]. Herein, the idea of a self-powered suspension is presented. It is shown that a substantial performance increase can be achieved with a relatively small amount of energy, using the correct actuation system. A related study is given in [5]. It describes an active suspension design, where the cabin is suspended by four air springs with electric actuators in parallel. Using a state transformation, which is found by optimization, the system is transformed to a roll-pitch-heave system which can be controlled more easily. The simulation results show that the vertical, roll and pitch accelerations can be reduced by 78%, 65% and 40% respectively. This is considerably more than expected, see for example [4]. However, the issue of attitude control is not considered at all. Furthermore, the precise decoupling is unclear and seems involved. Hence, the question remains, how to control the cabin of a commercial vehicle, considering both comfort and attitude behavior.

In this paper, a control strategy is presented for an active cabin suspension of a commercial vehicle, that significantly improves driver comfort without impairing the vehicle's pitch and roll behavior during extreme maneuvers. The suspension consists of 4 idealized 10 Hz bandwidth actuators below each of the cabin's corners. By means of input-output decoupling of the linearized equations of motion and the introduction of an active controller constraint, the system can be transformed into three decoupled Single-Input-Single-Output (SISO) loops. Each of these loops is controlled separately. The controller is evaluated using a number of simulations with a validated tractor semi-trailer simulation model. The controlled active suspension is shown to significantly enhance both driver comfort and attitude behavior. Additionally, the significance of adding passive damping is illustrated.

The paper is organized as follows. First, a cabin model is derived that is suitable for controller design. Next, the input-

Willem-Jan Evers, Igo Besselink and Henk Nijmeijer are with the Eindhoven University of Technology, Eindhoven, The Netherlands, W.J.E.Evers@tue.nl, I.J.M.Besselink@tue.nl, H.Nijmeijer@tue.nl. Arjan Teerhuis and Albert van der Knaap are with TNO Automotive, Helmond, The Netherlands, Arjan.Teerhuis@tno.nl. This research project is supported by TNO Automotive within the framework of the *Competence Centre for Automotive Research* (*CCAR*).

978-1-4244-4524-0/09/$25.00 ©2009 AACC

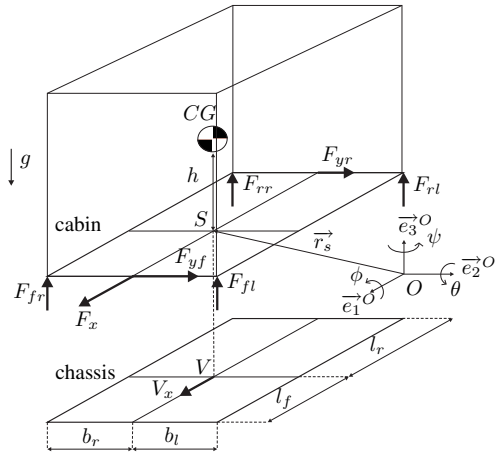

Fig. 1. Schematic representation of the control model.

output decoupling is addressed, followed by the controller design for each SISO-loop. Finally, the proposed controller is evaluated with a wide range of tests using a validated truck semi-trailer model.

II. Cabin model for controller design

The goal of this paper is to develop a controller for an active cabin suspension. Hereto, a model-based design is adopted. In virtue of subsequent control design, a model of limited complexity, which includes the main cabin dynamics, is desirable. The derivation of this model is considered in this section.

A schematic representation of the proposed model is given in Fig. 1. Herein, the cabin is modeled as a rigid body with the center of mass located at a certain height h above a point S on the bottom of the cabin. The point S is located at a length l_f from the front of the cabin and l_r from that of the rear. Furthermore, the distance to the left and right side of the cabin are b_l and b_r respectively. The bottom of the cabin is projected on the chassis, where the projection of S is V. V_x is the forward driving direction.

Assumption 1: Both chassis and cabin are assumed to behave as rigid bodies.

Even though the chassis may profoundly twist in reality, these flexibilities are not necessary for this simplified model.

Assumption 2: The motion of the chassis point V with respect to the fixed world point O is given, which is hence not influenced by the cabin suspension forces.

Four different coordinate frames are defined, see Fig. 1: an absolute frame in point O ($\underline{\overrightarrow{e}}^O$); a relative frame R in point O that follows the chassis rotations around the $\overrightarrow{e_3}^O$-axis; and a body-fixed frame in points V and S. Rotations ψ_s, ϕ_s and θ_s are called *yaw*, *roll* and *pitch* respectively. Furthermore, the subscript (s), which is used here as an example, indicates that the rotations are from the absolute frame O to the relative frame in S.

The cabin is suspended to the chassis by means of stiff spring-damper configurations in longitudinal ($\overrightarrow{e_1}^V$) and lateral ($\overrightarrow{e_2}^V$) direction. Additionally, in vertical ($\overrightarrow{e_3}^V$) direction a spring is positioned in parallel with an ideal force actuator, that has a bandwidth of 10 Hz, at each of the cabin corners. Therefore, the vertical suspension forces can be split into a force that originates from the passive suspension (F_{ij}^S) and one that is induced by the actuator (F_{ij}^A).

Assumption 3: The longitudinal ($\overrightarrow{e_1}^R$) and lateral ($\overrightarrow{e_2}^R$) movements of point S with respect to point V are negligible due to the high stiffness of the cabin suspension in those directions. Moreover $\psi_v - \psi_s = 0$, so both cabin and chassis follow the yaw-motions of the vehicle (ψ_r) exactly.

The longitudinal and lateral movements of the vehicle result in suspension forces acting on the cabin. These forces are depicted in Fig. 1 as F_x, F_{yf} and F_{yr}. Since the chassis motions are determined according to Assumption 2 and cabin motions according to Assumption 3, these longitudinal and lateral suspension forces can be deduced.

Assumption 4: $\frac{\delta}{\delta t}\underline{\overrightarrow{e}}^R = 0$ or negligible.

Assumption 4 holds as long as the yaw velocity of the vehicle is low. Under this assumption, $\underline{\overrightarrow{e}}^R$ can be considered as an absolute frame. In order to derive Lagrange's equations of motion, see for example [8], position vectors are needed. The position of the center of gravity of the cabin, point S and point V are given by

$$\begin{aligned}\overrightarrow{r_{cg}} &= [x\ y\ z]\underline{\overrightarrow{e}}^R \\ \overrightarrow{r_s} &= \begin{bmatrix} x - h\sin\theta_s \\ y + h\cos\theta_s\sin\phi_s \\ z - h\cos\theta_s\cos\phi_s \end{bmatrix}^T \underline{\overrightarrow{e}}^R \\ \overrightarrow{r_v} &= [x_v\ y_v\ z_v]\underline{\overrightarrow{e}}^R.\end{aligned} \tag{1}$$

Assumption 5: The suspension forces are all oriented along the principal axis of the frame $\overrightarrow{e}^R$.

Although this is not entirely in line with reality, this assumption is needed to keep the equations manageable. Moreover, the error that is introduced with this assumption is reasonably small under normal driving conditions.

Assumption 6: The angles $\phi_s,\ \theta_s,\ \phi_v$ and θ_v are small, hence the following approximations may be applied:

$$\begin{aligned}\cos\xi &\approx 1 \\ \sin\xi &\approx \xi \\ (\sin\xi)^2 &\approx 0.\end{aligned} \tag{2}$$

Assumption 6 holds under normal driving conditions. In case of driving on graded or strongly banked roads, a more complex model is required for accurate results. Under these assumptions, the following equations of motion are obtained:

$$\begin{bmatrix} m\ddot{z} \\ J_x\ddot{\phi}_s \\ J_y\ddot{\theta}_s \end{bmatrix} = \underbrace{TF^S}_{\underline{u}^S} + \underbrace{TF^A}_{\underline{u}^A} + \underline{w}, \tag{3}$$

where

$$\underline{T} = \begin{bmatrix} 1 & 1 & 1 & 1 \\ h\phi_s + b_l & h\phi_s - b_r & h\phi_s + b_l & h\phi_s - b_r \\ h\theta_s - l_f & h\theta_s - l_f & h\theta_s + l_r & h\theta_s + l_r \end{bmatrix}$$

$$\underline{w} = \begin{bmatrix} -mg \\ l_f\theta_s F_{yf} - l_r\theta_s F_{yr} + h(F_{yf} + F_{yr}) \\ l_f\phi_s F_{yf} - l_r\phi_s F_{yr} - (l_f\theta_s + h)F_x \end{bmatrix}$$

$$\underline{F}^S = \begin{bmatrix} F^S_{fl} & F^S_{fr} & F^S_{rl} & F^S_{rr} \end{bmatrix}^T$$
$$\underline{F}^A = \begin{bmatrix} F^A_{fl} & F^A_{fr} & F^A_{rl} & F^A_{rr} \end{bmatrix}^T. \quad (4)$$

Herein, $\underline{w}$ is a disturbance vector, $\underline{F}^A$ is a vector containing the actuator forces and $\underline{F}^S$ contains the forces from the passive suspension elements.

Using linear springs with stiffness c_s and linear dampers with damping constant d_s as passive suspension elements, the modal passive suspension inputs

$$\underline{u}^S = \underline{T}\underline{F}^S, \quad (5)$$

are given by

$$\underline{u}^S = -c_s\underline{G}_s \begin{bmatrix} z - z_v - h \\ \phi_s - \phi_v \\ \theta_s - \theta_v \end{bmatrix} - d_s\underline{G}_s \begin{bmatrix} \dot{z} - \dot{z}_v \\ \dot{\phi}_s - \dot{\phi}_v \\ \dot{\theta}_s - \dot{\theta}_v \end{bmatrix}, \quad (6)$$

where

$$\underline{G}_s = \begin{bmatrix} 4 & 2(b_l - b_r) & 2(l_r - l - f) \\ 2(b_l - b_r) & 2(b_l^2 + b_r^2) & b_l l_r - b_l l_f + \\ & & b_r l_f - b_r l_r \\ 2(l_r - l_f) & b_l l_r - b_l l_f + & 2(l_r^2 + l_f^2) \\ & b_r l_f - b_r l_r & \end{bmatrix}. \quad (7)$$

III. Input-Output decoupling

In this section, an approach is proposed to determine a suitable control strategy based on the equations of motion, as given in (3). A key observation from (7) is that the heave (z), pitch (θ_s) and roll (ϕ_s) dynamics are coupled through the interaction from the suspension elements. In addition, each actuator force affects all of these modes, see (4). Moreover, there are four control inputs and only three outputs, hence the system is over-actuated. To deal with interaction and over-actuation, input-output decoupling is investigated.

Assumption 7: The absolute cabin orientation $(\theta_s, \phi_s, \psi_s)$ cannot be measured or estimated accurately. Therefore, these angles are not available for control. Consequently, these angles are assumed zero where needed.

From (3), it is known that the vector of modal actuator inputs is given by

$$\underline{u}^A = \underline{T}\underline{F}^A. \quad (8)$$

As $\underline{T}$ is not a square matrix, $\underline{F}^A$ cannot be uniquely determined given a certain $\underline{u}^A$. One way of finding a unique transformation is by looking for an additional constraint. For this purpose, a dynamically inspired choice is available:

$$F^A_{fr} + F^A_{rl} - F^A_{rr} - F^A_{fl} = 0. \quad (9)$$

In practice, assumption 7 will not hold, as the cabin floor is flexible to some extend. If the actuators are used to twist the cabin floor, energy is being wasted and cabin fatigue issues may be the result, hence this has to be prevented. Combining (3), (4) and (9) under Assumption 7 gives

$$\underline{F}^A = \tilde{\underline{T}}^{-1} \begin{bmatrix} \underline{u}^A \\ 0 \end{bmatrix}$$
$$\tilde{\underline{T}}^{-1} = \begin{bmatrix} 1 & 1 & 1 & 1 \\ b_l & -b_r & b_l & -b_r \\ -l_f & -l_f & l_r & l_r \\ -1 & 1 & 1 & -1 \end{bmatrix}^{-1}, \quad (10)$$

which is an invertible transformation as $(b_l,\ b_r,\ l_f,\ l_r) > 0$. An alternative way, to find a unique transformation is by using the so-called pseudo-inverse (or *Moore-Penrose inverse*), see [6]. For our system, the pseudo-inverse, which is optimal in a least-square sense, is given by

$$\underline{T}^\dagger = \underline{T}^T(\underline{T}\underline{T}^T)^{-1}. \quad (11)$$

It can be easily checked that

$$\tilde{\underline{T}}^{-1} = \begin{bmatrix} \underline{T}^\dagger, & \underline{\star} \end{bmatrix}, \quad (12)$$

with $\underline{\star}$ some vector that has no influence on the transformation, due to the zero input in (10). Hence, both approaches give the same unique relation.

The next step is to overcome the interaction that is caused by the passive suspension forces, that is, the forces resulting from the non-diagonal terms in (7). Only the spring related terms are compensated, as the damper related terms merely dissipate energy. Hence, compensating for the non-diagonal damper terms would not be energy efficient. As a result, the modal actuator inputs become

$$\underline{u}^A = c_s\tilde{\underline{G}}_s \begin{bmatrix} z - z_v - h \\ \phi_s - \phi_v \\ \theta_s - \theta_v \end{bmatrix} - \tilde{w} + \underline{u}^C, \quad (13)$$

with $\underline{u}^C$ the vector of modal controller inputs and

$$\tilde{\underline{G}}_s = \begin{bmatrix} 0 & 2(b_l - b_r) & 2(l_r - l - f) \\ 2(b_l - b_r) & 0 & b_l l_r - b_l l_f + \\ & & b_r l_f - b_r l_r \\ 2(l_r - l_f) & b_l l_r - b_l l_f + & 0 \\ & b_r l_f - b_r l_r & \end{bmatrix}. \quad (14)$$

The disturbances are approximated as

$$\tilde{\underline{w}} = \begin{bmatrix} -mg \\ hm\hat{\ddot{y}}_v \\ hm\hat{\ddot{x}}_v \end{bmatrix} \quad (15)$$

with h as given in Fig. 1 and $\hat{\ddot{x}}_v,\ \hat{\ddot{y}}_v$ the longitudinal and lateral acceleration of the chassis respectively filtered with a

10 Hz first order low-pass filter. Consequently, the decoupled equations of motion become

$$\begin{bmatrix} m\ddot{z} \\ J_x\phi_s \\ J_y\theta_s \end{bmatrix} = \underline{u}^C - c_s(\underline{G}_s - \underline{\tilde{G}}_s) \begin{bmatrix} z - z_v - h \\ \phi_s - \phi_v \\ \theta_s - \theta_v \end{bmatrix} + \underline{\epsilon}, \tag{16}$$

with $\underline{\epsilon}$ an error term that is assumed negligible. Using these assumptions and equations, the input-output behavior is decoupled. In the next section, the design of a control strategy for each of the decoupled loops is addressed.

IV. Control strategy

By means of the input-output decoupling as described in the previous section, a system consisting of three independent SISO-loops has been derived. The control objective differentiates between two different disturbances. On the on hand, there are driver induced disturbances, for example when braking, accelerating or cornering. In these cases, the cabin attitude behavior should mimic the chassis motions, for an optimal handling feeling. Note that this is (for a large part) achieved by the compensation term $\tilde{w}$ in (13). On the other hand, there are disturbances originating from the road. These need to be suppressed to some extent, depending on the available working space and the intensity of the disturbances. The objective in this case is to minimize the ISO weighted cabin accelerations. This is reflected in the ride comfort index, which consists of the sum of ISO frequency weighted accelerations [9],

$$RCI = \sqrt{\frac{1}{T}\int_0^t (\ddot{x}_{ISO}^2 + \ddot{y}_{ISO}^2 + \ddot{z}_{ISO}^2)\, dt}, \tag{17}$$

hence the lower the RCI value, the better the comfort perceptence.

The standard control approach for vibration mitigation, which is optimal - with respect to root-mean-square suspension deflections and suspended mass acceleration - for a single suspended mass with white noise disturbance velocity, [7], is the use of a stiffness in combination with *skyhook damping*. In practical application additional low-frequent leveling (integral action) is often desirable, for example when driving uphill [14]. As such, the controller is given by

$$\underline{u}^C = \begin{bmatrix} -I_z \int_0^t (z - z_v - h)dt - \\ (c_z - 4c_s)(z - z_v - h) - d_{sky}^z \dot{z} \\ \\ -I_\phi \int_0^t (\phi_s - \phi_v)dt - \\ (c_\phi - 2c_s(b_l^2 + b_r^2))(\phi_s - \phi_v) - d_{sky}^\phi \dot{\phi}_s \\ \\ -I_\theta \int_0^t (\theta_s - \theta_v)dt - \\ (c_\theta - 2c_s(l_f^2 + l_r^2))(\theta_s - \theta_v) - d_{sky}^\theta \dot{\theta}_s \end{bmatrix}, \tag{18}$$

with $I_z,\ I_\phi,\ I_\theta,\ c_z,\ c_\phi,\ c_\theta,\ d_{sky}^z,\ d_{sky}^\phi,\ d_{sky}^\theta$ the controller parameters.

Remark 8: While the symmetric and asymmetric road inputs can be considered to be uncorrelated when driving a vehicle in practice, the disturbances $\dot{z}_c$ and $\dot{\theta}_c$ are correlated. Moreover, all disturbances (also $\dot{\phi}_c$) will be filtered white noise. As such the controller structure as given in (18) will not be optimal. However, it is considered a good starting point for more advanced controller design research.

TABLE I
Vehicle simulation parameters

Parameter	Magnitude	Unit	Parameter	Magnitude	Unit
l_f	0.94	m	I_z	200000	Nm/s
l_r	1.14	m	I_ϕ	70000	Nm/s
b_l	0.56	m	I_θ	100000	Nm/s
b_r	0.56	m	c_z	240000	N/m
h	0.97	m	c_ϕ	200000	N/rad
m	1300	kg	c_θ	200000	N/rad
J_x	1100	kgm^2	d_z	35000	Ns/m
J_y	1100	kgm^2	d_ϕ	40000	Ns/rad
c_s	60000	N/m	d_θ	50000	Ns/rad
d_s	0 or 4000	Ns/m			

V. Evaluation

To evaluate the proposed controller, the validated (44 DOF) tractor semi-trailer model as described in [2] is used. The model is implemented in *Matlab/SimMechanics*, which is the multi-body toolbox of *Matlab/Simulink*. The cabin suspension of the vehicle model is modified in the following way: the (front) roll stabilizer between the cabin and chassis is removed and four actuators are placed beneath the cabin mounts. These actuators are modeled as ideal force actuators that act on both cabin and chassis, with a limited bandwidth of 10 Hz, which is modeled using a first order low-pass filter. Furthermore, two scenarios are evaluated to investigate the importance of passive damping. Firstly, the passive damping (d_s) is reduced to zero. Secondly, it is reduced to approximately 60% of that of a passive steel sprung suspension design. The relevant cabin parameters are given in Table I.

The controller parameters are the result of manual tuning. A reasonably high passive spring stiffness is selected, since it is desirable to avoid the bump-stops without the requirement of very strong passive dampers that deteriorate the high frequent comfort. The skyhook damping terms are tuned to get a sufficient comfort improvement under normal driving conditions. Furthermore, the passive damping is chosen such that the bump-stops do not deteriorate comfort, when traversing a symmetric road bump - as described later on - at 20 km/h. Moreover, the integrator gains are selected such that the cabin levels in under 5 seconds.

A. Steady-state I/O-test

Firstly, the quality of the input-output decoupling is verified. Hereto, a step-shaped signal is added to the modal control inputs and the cabin response is evaluated. A step in the first, second and third element of $\underline{u}^C$ is applied at time $t = 10$, $t = 15$ and $t = 20$ seconds respectively. The response when the vehicle is at standstill is given in Fig. 2 for small inputs (a) and larger inputs (b). The decoupling is very accurate for roll and pitch moments, since each of the inputs only affects the related state component. However, for vertical force inputs, the first element of $\underline{u}^C$, a small amount of interaction is still visible. When comparing the results for small and big inputs, it can be seen that the amount of

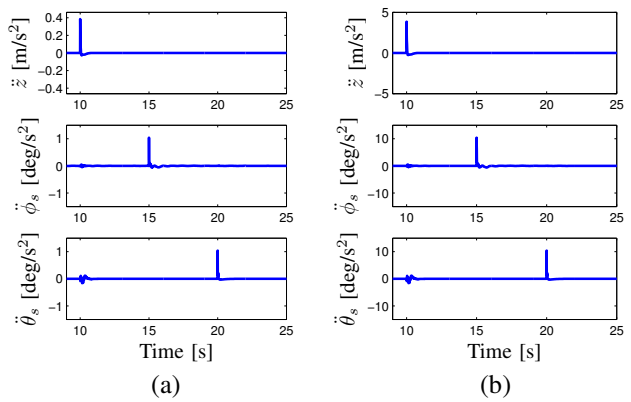

Fig. 2. Input-output evaluation at standstill ($d_s = 4000$): cabin vertical acceleration (top); roll acceleration (mid); pitch acceleration (bottom). Relatively small input steps (a), relatively large input steps (b).

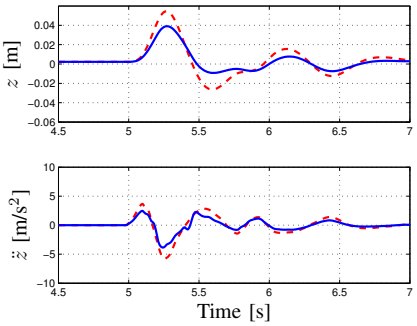

Fig. 3. Symmetric bump test, cabin heave response: passive air suspension (dashed); active suspension (solid).

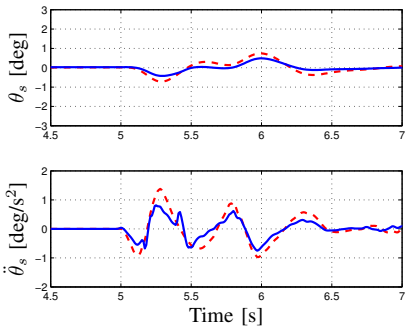

Fig. 4. Symmetric bump test, cabin pitch response: air suspension (dashed); active suspension (solid).

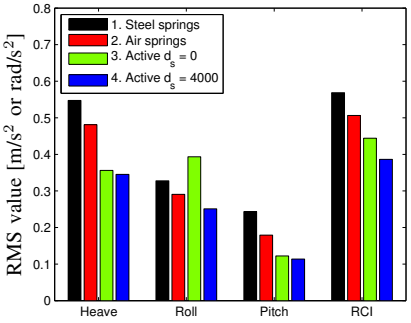

Fig. 5. Overview of comfort evaluation on asphalt.

interaction remains nearly the same. Consequently, as the method appears valid for the full working range, the results are satisfactory.

B. Symmetric bump test

The second simulation test consists of driving over a symmetric trapezoidal bump (both left and right wheels have the same road profile) with a constant velocity of 20 km/h. The bump has a length of 1.4 m, and a height of 0.06 m. The upward and downward slopes are each 0.6 m in length. The control objective is to avoid the bump-stops, while minimizing pitch and heave accelerations. However, even though the bump has a realistic shape, the bump-stops could not be avoided without adding passive damping or increasing the stiffness to undesirable high values. The heave and pitch response using $d_s = 4000$ Ns/m are given in Fig. 3 and 4 respectively. The dashed line gives the response for a conventional (soft) air sprung suspension, and the solid line gives the response using the proposed active suspension.

Overall, it can be seen that the active suspension significantly reduces the accelerations. There is a 32% decrease in ride comfort index (comfort increase) with respect to the passive air suspended cabin. However, there are also some small spikes visible - at 5.2 and 5.4 seconds - where the bump-stops are touched. Hence, if the minimum requirement is increased, for example that this bump needs to be taken at 30 km/h, additional passive damping is required to avoid the bump-stops. Alternatively, stroke dependent damping is worthwhile to investigate, see for example [15]. However, this is beyond the scope of this paper.

C. Comfort evaluation on asphalt

For the comfort evaluation a measured road profile is used, corresponding to a stretch of reasonably smooth asphalt. This road is traversed with a constant velocity of 85 km/h, using several cabin suspension configurations. An overview of the results is given in Fig. 5.

Firstly, Fig. 5 confirms a well known fact: lowering the stiffness by replacing the steel sprung suspension with an air sprung suspension improves comfort (11% in this simulation). Furthermore, the significant gain using an active suspension is also clear. Remarkably, the decrease in ride comfort index (comfort increase) is largest for the configuration with added passive damping: 25% with respect to the passive air suspension. The explanation lies in the roll behavior, see Fig. 6.

The vehicle has two resonances (9 and 20 Hz), which require a significant amount of damping. Given the limited bandwidth of our actuator (10 Hz) these need to be covered by adding passive damping. If this is not addressed, significant discomfort results. On the other hand, the effect of removing the passive roll stabilizer (in combination with the added skyhook damping) can also be seen. The power spectral density dropped significantly in the range of $0.5 - 3$ Hz.

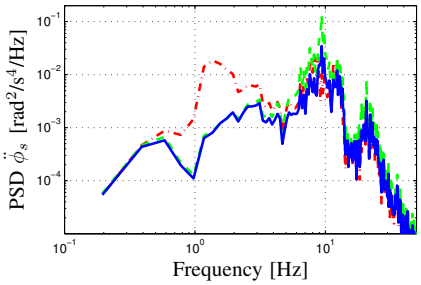

Fig. 6. Comfort evaluation on asphalt, power spectral density roll acceleration: air suspension (dash-dotted); active suspension $d_s = 0$ (dashed); active suspension $d_s = 4000$ (solid).

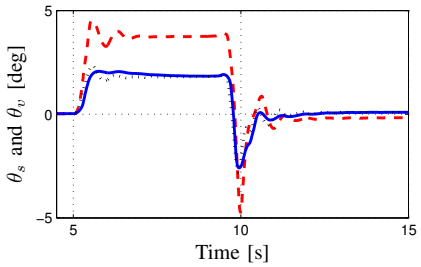

Fig. 7. Emergency braking, absolute pitch angle: cabin - air suspension (dashed); cabin - active suspension $d_s = 4000$ (solid); chassis (dotted).

D. Emergency braking

The emergency braking procedure is a safety critical event, where starting at a constant velocity of 85 km/h, the brakes are fully applied at time $t = 5$ seconds. The mean deceleration is approximately 5 m/s^2. The pitch response is given in Fig. 7. It is observed that while the air suspension dives into the bump-stops, the active suspension smoothly follows the chassis movements. Moreover, the large oscillation when coming to a complete standstill at $t = 10$ seconds (the reason why truck drivers release the brake just before that moment) is also significantly reduced.

E. Double lane-change

As final simulation, a double lane-change maneuver is simulated, with a maximal lateral acceleration of approximately 2 m/s^2. The roll response is given in Fig. 8. The passive air sprung suspension has a much higher roll stiffness, which results in a very strong coupling between chassis and cabin roll. With the active suspension, the cabin response shows some overshoot as a result of the integral action. However, this is expected to be acceptable.

VI. Conclusions and Future Work

A new control strategy is presented for an active cabin suspension of a commercial vehicle. Using input-output decoupling it is shown that the MIMO system can be transformed into three SISO loops. Each of these loops is controlled using skyhook damping with an added stiffness and integral action for low frequent leveling. Furthermore, to eliminate cabin roll and pitch when cornering and braking/accelerating a compensation strategy is added. It is shown by means of a number of simulations with a validated (44 DOF) tractor semi-trailer model that the controller meets its objectives. Moreover, it is shown that adding passive damping is highly desirable for driver comfort.

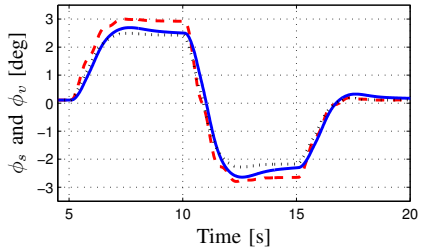

Fig. 8. Double lane-change, absolute roll angle: cabin - air suspension (dashed); cabin - active suspension $d_s = 4000$ (solid); chassis (dotted).

For future research an improved actuator model is desirable to obtain insight in the power requirements. Analysis of the mechanical power required by the proposed controller when driving on smooth asphalt (section VC), showed power peaks of 3.5 kW (average of 0W: flat road). Consequently, the power usage is expected to be an important evaluation aspect. Moreover, it might also be interesting to evaluate the possibilities and driver acceptance of eliminating cabin roll and pitch while cornering, braking and accelerating.

References

[1] Cole, D.J. "Fundamental Issues in Suspension Design for Heavy Road Vehicles". *Vehicle System Dynamics*, 35(4), pp 319-360, 2007.

[2] Evers, W.-J., Besselink, I., van der Knaap, A. and Nijmeijer, H. "Development and validation of a modular simulation model for commercial vehicles". *Int. Journal of Heavy Vehicle Systems*, accepted for publication in 2009.

[3] Evers, W.-J., Besselink, I., van der Knaap, A. and Nijmeijer, H. "Analysis of a variable geometry active suspension". *Int. Symposium on Advanced Vehicle Control*, Kobe, Japan, pp 350-355, 2008.

[4] Fisher, D. and Isermann, R. "Mechatronic semi-active and active vehicle suspensions". *Control Engineering Practice*, 12, pp 1353-1367, 2004.

[5] Graf, C., Maas, J. and Pflug, H.-C. "Konzept für eine aktive Lkw-Fahrerhauslagerung". *AUTOREG 2008 Conference*, Baden-Baden, Germany, February 2008, (written in German).

[6] Ben-Israel, A. and Greville, T.N.E. "Generalized Inverses: Theory and Applications". Wiley-Interscience, 1974.

[7] Hrovat, D. "Survey of advanced suspension developments and related optimal control applications". *Automatica*, 33(10), pp 1781-1817, 1997.

[8] Huston, R.L. "Multibody dynamics". ISBN: 0-409-90041-9, Butterworth-Heinemann, London, 1995.

[9] International Standard ISO 2631-1:1997. "Evaluation of human exposure to whole-body vibration - Part 1: General requirements", 1997.

[10] Jones, W.D. "Easy ride: Bose Corp. uses speaker technology to give cars adaptive suspension". *IEEE Spectrum*, 42(5), pp 12-14, 2005.

[11] Nakano, K., Suda, Y., Nakadai, S. and Tsunashima, H. "Self-powered active control applied to a truck cab suspension". *JSAE Review*, 20(4), pp 511-516, 1999.

[12] Nakano, K. and Suda, Y. "Combined Type Self-Powered Active Vibration Control of Truck Cabins". *Vehicle System Dynamics*, 41(6), pp 449-473, 2004.

[13] Roebuck, R.L., Cebon, D., Jeppesen, B.P. and Haque, J. "A systems approach to controlled heavy vehicle suspensions". *Int. Journal of Heavy Vehicle Systems*, 12(3), pp 169-192, 2005.

[14] Youn, I., Im, J. and Tomizuka, M. "Level and attitude control of the active suspension system with integral and derivative action". *Vehicle System Dynamics*, 44(9), pp 659-674, 2006.

[15] Venhovens, P.J.Th. "Optimal Control of Vehicle Suspensions". *Ph.D. Thesis*, Delft University of Technology, 1993.